Hybrid Nanoparticles

DOI: 10.1002/anie.201006407

Synthesis and Photocatalytic Properties of a Family of CdS-PdX Hybrid Nanoparticles**

*Yossi Shemesh, Janet E. Macdonald, Gabi Menagen, and Uri Banin**

Developing the composition and morphological control of hybrid nanoparticles is an intense area of recent research.[1] Nanoparticles containing disparate materials are of interest for applications such as magnetically separable catalysts,[2] photocatalysts,[3] biological imaging,[4] electronic components,[5] and photovoltaics.

Many combinations of magnet–metal,[6] magnet–semiconductor,[2,7,8] and semiconductor–metal[8] nanoparticles have been prepared, but of particular interest herein are hybrids incorporating the cadmium chalcogenide semiconductors, which have size dependent tunable band gaps in the visible region and well established chemistry and morphological control at the nanoscale. Hybrids of CdS and CdSe nanorods with Au,[9,10] Pt,[11–13] FePt,[7] NiPt, CoPt,[14] and Co[2] have been reported, with some control over the location of the metal growth, whether it be at a single tip,[9,10] both tips,[15] defect sites along the nanorod body,[9,11,12] or adjacent to a seed location.[9,11,16] The metal regions have been used as target sites for self assembly[17] and electrical contacts.[5] Moreover, the metal islands can serve as acceptors for electrons following a light-induced charge separation process.[3,18,19] This is a necessary component for photocatalysis and photovoltaics, and several of these hybrids of CdS have shown to photoreduce water.[3,13,19] These early successes indicate there are many more possibilities for interesting material combinations and morphologies in hybrid semiconductor nanoparticles for application developments.

In the preparation of metal–semiconductor hybrid nanoparticles, it is important to consider their intended use and inherent stability. For many of the aforementioned applications, the hybrids will be exposed to oxidizing environments such as air and water. In the case of hybrids with CdS, the second component is directly in contact with the sulfidizing environment of the semiconductor. Hybrids of CdS with metal sulfides and oxides may maximize chemical stability in these environments.

Palladium is one of the most important transition metals because of its exceptional catalytic properties. For example, palladium oxide has been widely reported as the catalyst of choice in methane combustion[20,21] and is also efficient in liquid phase oxidations of alcohols.[22] In contrast, the palladium sulfides have long been ignored for their catalytic properties and usually regarded as undesirable products after the poisoning of metallic palladium by hydrogen sulfide.[23] Yet recent research has begun to recognize the catalytic potential of the palladium sulfides, since they are chemically very stable. Pd_4S, a conductor,[24] has become a candidate for replacing Pd^0 in electrodes in which extreme chemical, pH, and temperature stability is required.[25] It is with this stability and catalytic activity in mind that hybrid nanoparticles of cadmium sulfide with palladium sulfide and palladium oxide are targeted products.

Herein we study the synthesis, under very different reaction conditions, of two types of hybrid nanoparticles of CdS with palladium compounds (Scheme 1). CdS-Pd_4S was

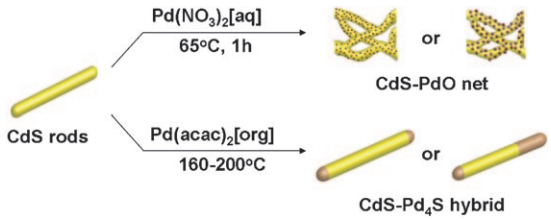

Scheme 1. Synthetic routes to hybrid nanoparticles of CdS nanorods and palladium compounds. acac = acetylacetonate.

achieved through high-temperature organic-phase synthesis,[14] and CdS-PdO was synthesized by the aqueous condensation of Pd^{II} onto CdS nanorods.[12] Both of these materials were also tested and compared for their function in the photocatalytic reduction of water.

CdS nanorods of varying diameters were prepared by the seeded-growth method (Figure S1 and Table S1 in the Supporting Information).[26] The synthesis of CdS-Pd_4S hybrid nanoparticles was achieved by injecting a solution of CdS nanorods into a solution of palladium(II) acetylacetonate in oleylamine and oleic acid at 200 °C. TEM images (Figure 1 a–d) indicate a product that maintains the shape and narrow size distribution of the initial CdS nanorods, but there are areas that show greater contrast at one or both tips of the nanorods. These dark areas were presumed to be Pd containing regions of the nanorods. HRTEM images (Figure 1 d) of a single

[*] Y. Shemesh, Dr. J. E. Macdonald, G. Menagen, Prof. U. Banin
Institute of Chemistry and the Center for Nanoscience and Nanotechnology, The Hebrew University of Jerusalem, Jerusalem, 91904 (Israel)
Fax: (+972) 2-658-4148
E-mail: banin@chem.ch.huji.ac.il
Homepage: http://chem.ch.huji.ac.il/~nano/

[**] Supported in part by the Israel Science Foundation (grant 972/08) and the ERC Advanced Investigator Project DCENSY (grant 246841). U.B. thanks the Alfred and Erica Larisch Memoral Chair in Solar Energy. We thank Dr. Vitaly Gutkin and Dr. Inna Popov from the Harvey M. Krueger Family Center for Nanoscience and Nanotechnology for their assistance with XPS and TEM, and Amit Sitt for his assistance with graphics.

Supporting information for this article is available on the WWW under http://dx.doi.org/10.1002/anie.201006407.

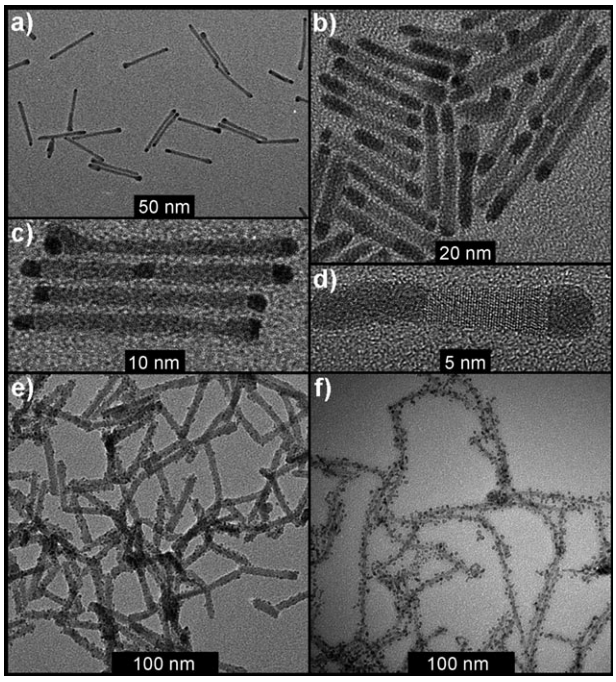

Figure 1. CdS-X hybrid nanostructures: a) tip growth of Pd_4S on 5.9 nm diameter nanorods; b) more extensive growth of Pd_4S on a sample of CdS nanorods with a broad size distribution; c) close-up of the sample shown in (a); d) HRTEM of a single CdS-Pd_4S nanorod from the sample shown in (b); e) CdS nanonets composed of 7.1 nm diameter nanorods decorated with small PdO dots; f) thin rods of 4.5 nm diameter grew large dots of PdO.

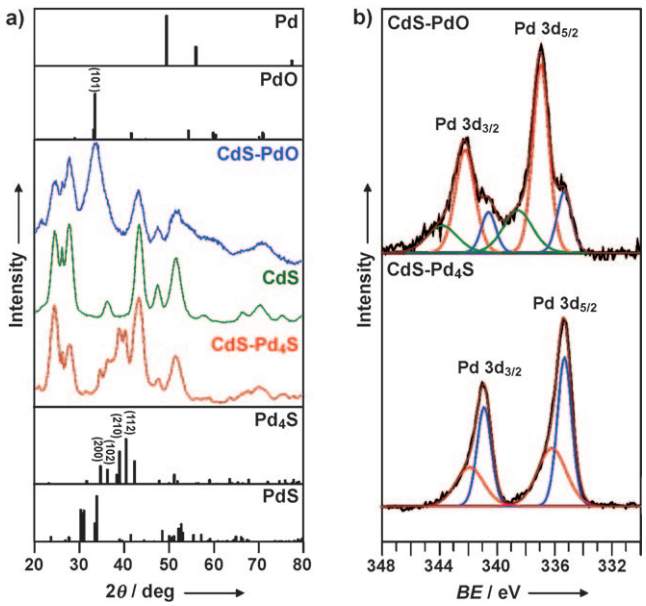

Figure 2. a) XRD data of CdS-PdX hybrid nanostructures. The continuous color lines at the middle show the experimental data of CdS nanorods and the synthesized hybrid structures. The black lines represent the expected positions and relative intensities of reflections from Pd (JSPDS 00-246-1043), PdO (JSPDS 00-041-1107), Pd_4S (JSPDS 04-007-4312), and PdS (JSPDS 04-007-0708); b) High-resolution XPS in the Pd 3d spectral region of the hybrid nanoparticles. The experimental data (black) were fitted to Pd^0 (blue), Pd^{II} (red), and Pd^{IV} (green).

particle shows that the lighter areas maintain the lattice fringes indicative of the CdS nanorod, but these do not extend into the dark areas.

In contrast, synthesis of Pd-containing hybrids in aqueous solution yielded different products. The CdS nanorods were first rendered water soluble by ligand exchange to 1-mercaptoundecanoic acid (MUA). Palladium(II) nitrate was then added to the nanorods at 65 °C, which yielded an extended nanonet of CdS nanorods[12] decorated along the rod bodies with dots of palladium-containing product (Figure 1 e,f).

The powder X-ray diffraction (XRD) pattern (Figure 2) of the decorated nanonets allowed identification of the Pd product. Clear reflections of the CdS component of the hybrid were observed. A strong broad peak appeared at 33.8° and was identified as the PdO (101) reflection. At larger angles, the PdO contribution to the pattern can also be seen at 54.7°, 60.5°, and 71.5°. The broadness of the peak indicates small crystallites of the PdO phase, which is consistent with the small dots observed by TEM. X-ray photoelectron spectroscopy (XPS) (Figure 2) supports the assignment of PdO as the binding energy of the strongest peak at 336.9 eV is indicative of Pd^{II}. In the XRD pattern, no peak from crystalline Pd metal was seen at 40.1°, yet XPS data shows small amount of Pd^0 at a binding energy of 335.3 eV. This peak was assigned to the decomposition of PdO and is common in preparations of PdO nanoparticles.[21] Both of these energies agree very well to values seen previously for PdO nanoparticles.[27] We also observed a higher binding energy peak at 338.52 eV, which can be assigned to the oxidation state of Pd^{IV}, and is likely due to the presence of amorphous PdO_2[28] or other higher oxidized palladium species such as surface oxyhydroxides.

The mechanism of PdO formation likely involves Pd^{II} hydrolysis to palladium hydroxide, followed by condensation and nucleation of PdO.[29] This mechanism is supported by the slight lowering of the pH value of the solution as the reaction progressed. Heterogeneous nucleation of PdO on the nanorods formed the CdS-PdO hybrid with 1–3 nm PdO dots dispersed on the nanorod bodies.

Interestingly, a dependence on nanorod thickness was found in the aqueous synthesis (Figure 1 e,f). Synthesis with thin nanorods ($d = 4.5$ nm) led to growth and decoration with large PdO dots of 2.7–3.3 nm. Thicker nanorods ($d = 6.0$ nm) under the same reaction conditions gave PdO dots of 1.6–2.0 nm, while even thicker nanorods ($d = 7.1$ nm) led to the growth of very small dots of only 0.8–1.2 nm. Increasing the amount of palladium precursor sixfold did not give a noticeable change in the size of the dots (Figure S4 in the Supporting Information). We suggest this change in size is due to ligation and stabilization by the carboxylic acid groups of MUA. On thicker nanorods, because of the lower radius of curvature, more acid head groups are able to bend and ligate the PdO dots, thus stabilizing the smaller sizes. On thinner nanorods, the small radius of curvature and the higher density of surface defects prevents the efficient packing of the MUA, lowering the surface density of carboxylic acid groups to ligate the PdO nanoparticles.

Contrary to the aqueous synthesis, the identification of the Pd component of the product of the high-temperature synthesis indicated hybrid formation through an entirely different mechanism. The XRD pattern of the hybrids shows strong reflections due to CdS and several peaks in the range of 30–40°, where no strong reflections are expected for CdS (Figure 2). Palladium and sulfur have six different polymorphs, but the window at 30–40° provides sufficient detail to identify reflections matching the bulk pattern of Pd_4S. Of particular note, there are no reflections due to PdS, which would have been expected from a direct ion-exchange-type reaction (see below).

Further confirmation for the assignment of Pd_4S is provided by XPS results presenting a strong Pd^0 peak and a smaller Pd^{II} peak at 335.3 eV and 336.1 eV, respectively.[30] The ratio between the Pd^0 and the Pd^{II} peaks was closer to 1.3:1 than 3:1 as is expected from the stoicheometry of the palladium sulfide. Previous calculations and experimental results show Pd_4S to have sulfur-enriched surfaces.[31] Correspondingly, we observed a larger ratio of Pd^{II} because of the large surface to volume ratio provided by the nanoparticle sample.

The initial characterization did not provide enough evidence to indicate whether the Pd_4S forms a shell on the nanorods or extends through the core (Figure 1 a–d). To address this question, high-angle annular dark field–scanning TEM (HAADF-STEM) and energy-dispersive X-ray spectroscopy (EDS) analysis were employed, as demonstrated on one of the particles from the sample seen in Figure 1 b (Figure 3). EDS spectra were collected from two areas on the same CdS-Pd_4S hybrid giving their elemental makeup. The brighter area showed a large peak due to palladium, and conversely the darker area showed a large peak due to cadmium. Importantly, almost no Cd was seen in the Pd-rich area and vice versa. Therefore, we concluded that the Pd_4S exchanges throughout the thickness of the nanorod.

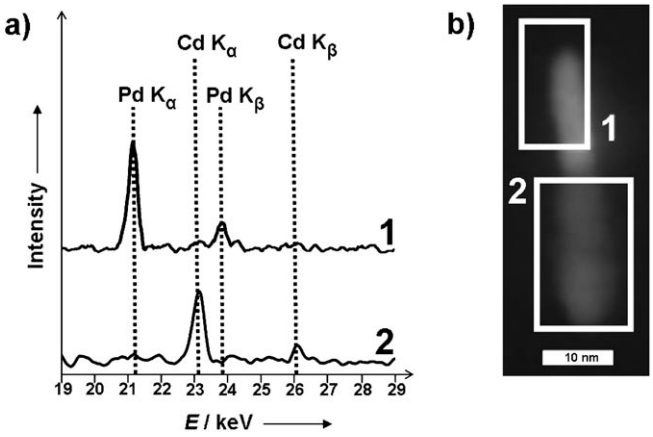

Figure 3. HAADF-STEM image of the hybrid structures. a) EDS elemental analysis of the highlighted areas of a single CdS-Pd_4S nanorod shown in (b).

The reaction of Pd^{II} with the CdS nanorods to yield CdS-Pd_4S hybrid nanoparticles appears to be a partial cation-exchange reaction. In cation-exchange reactions, such as the conversion from CdS into Cu_2S or CdS into Ag_2S,[32,33] nanorods are stirred in a solution of the new cation, and the Cd^{II} is leached out and replaced with the new cation while the sulfur anions remain in place. The shape and size of the original particles are retained in the product. In the present case, the size and shape of the hybrid nanoparticles is similar to the original nanorods, and the product has palladium sulfide regions replacing what was originally CdS volume in the nanorods.

Despite the resemblance to traditional cation exchange, there is an outstanding difference in the formation of CdS-Pd_4S. In a direct exchange of Cd^{II} and Pd^{II}, PdS would be the expected product. Instead Pd_4S forms, which contains palladium in both the II and 0 oxidation states. Furthermore, Pd_4S has a less negative enthalpy of formation than PdS[34] and so is neither the expected thermodynamic product. Clearly, the role of the surfactants and interfacial energies cannot be neglected in these reactions.

Long-chain amines are known to reduce palladium(II) at elevated temperatures.[35] Indeed, an observed by-product of this reaction was free Pd^0 nanoparticles, which were removed during purification. Reduction of the palladium precursor by amines is the likely source of Pd^0 in the sulfide. There was no evidence of metallic palladium particles nucleating heterogeneously on the nanorods, and, therefore, there must be a second force driving the formation of Pd_4S. In some cation-exchange processes it is necessary to add ligands to bind the outgoing cations to drive the reaction.[33] In the present case, when oleic acid was not present, Pd_4S did not form. Oleic acid is known to strongly ligate Cd^{II},[36] and its role may be to help thermodynamically drive the exchange process. We propose that the particular combination of reducing and Cd^{II} ligating surfactants is a necessary factor in the formation of Pd_4S-CdS hybrid nanorods and that the reaction is a unique process of simultaneous reduction and cation exchange to yield an unanticipated product.

Two regimes were noted in the growth of the CdS-Pd_4S hybrid structures presented: one in which the Pd only exchanges at the tips of the nanorods (Figure 1 a,c) and the second in which the exchange is more extensive and growth into the bodies of the nanorods is observed (Figure 1 b,d). The exchange to Pd_4S occurs from the ends of the nanorods and is similar in that manner to the exchange of CdS to Cu_2S,[32] for which the growth mode minimizes the interfacial energy of the two regions to lower the energy of formation. The growth is often more extensive from one end than the other, and is likely due to the different reactivity of the crystallographically anisotropic ends of the wurtzite CdS nanorods.[9,32]

The Pd_4S exchange depends on the diameter of the rods. Whereas thinner nanorods show reactivity towards Pd, thicker 7 nm diameter nanorods showed almost no exchange to Pd_4S (Figure S5 in the Supporting Information). We postulate that the small radius of curvature at the tips of small diameter rods provide reactive, high-energy surfaces not present for rods of larger diameter. Combined with the observation of tip-directed growth, this result provides further evidence that the exchange reaction is only slightly thermodynamically favored, as it only occurs in areas of high energy

and small radius-of-curvature, namely tips and thin regions of the nanorods.

The coupling of palladium compounds to CdS is of interest for their electronic band misalignments, which can be exploited and tailored for applications such as photocatalysis. In this process, light is absorbed in the semiconductor segment forming an exciton. This is followed by charge separation whereby an electron transfers from the semiconductor to the lower energy levels of the secondary material and leaves behind a hole. We studied photoinduced charge separation in the CdS-PdX hybrids through the photoreduction of water to yield hydrogen gas, which is quantifiable by gas chromatography (Figure 4).

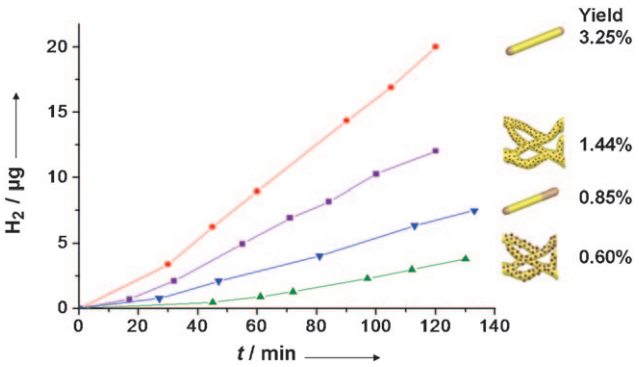

Figure 4. Photocatalytic H_2 production by CdS-PdX hybrids in an aqueous solution of sulfide and sulfite[19] and excited at $\lambda = 405$ nm. Experiments were performed at the limit whereby nearly all the photons are absorbed by the sample. Yields relate H_2 formation to the number of photons absorbed. ● CdS-Pd_4S tip exchange; ■ CdS-PdO small dots; ▼ CdS-Pd_4S body exchange; ▲ CdS-PdO large dots. Control experiments of CdS nanorods and Pd nanoparticles gave yields of 0.03% and 0.003%, respectively. Hydrogen evolution was not detected for PdO nanoparticles without CdS.

CdS-PdO hybrid nanoparticles with smaller PdO dots show 2.5 times higher photocatalytic activity over those with larger dots, despite the latter presenting more total palladium and more exposed surface area of the PdO per cadmium unit (see the Supporting Information). This result is consistent with earlier results on similar CdSe-Pt decorated nanonets for the photocatalytic reduction of methylene blue, whereby hybrids with smaller Pt clusters showed greater reactivity.[12]

Undesired absorbance of the incident photons by the PdO regions, which does not lead to charge separation, is a likely source of decreased efficiency. Indeed, for the CdS-PdO hybrids with large PdO dots, it was calculated that PdO accounts for 63% of the measured absorbance at the specific excitation wavelength of 405 nm, whereas PdO accounts for only 28% of the absorbance in the hybrid with the small dots (see the Supporting Information). However, this phenomenon is unlikely to explain all of the 2.5 fold increase in activity for the hybrid with the small dots.

It is possible that the small PdO dots are inherently more catalytically active as has been shown for other small nanoparticles, such as gold.[37] Through quantum confinement, smaller semiconductor PdO dots may have elevated conduction band energy level, thus making the reduction of the water more thermodynamically favorable and increasing yields. The small particles may also present a greater number of reactive step-edge sites, increasing their catalytic activity.

For the Pd_4S-CdS hybrids, nanorods with a small amount of tip exchange were four times more efficient at producing H_2 than catalysts with more extensive Pd_4S exchange. Parasitic absorbance by the Pd_4S regions is also a contributing factor, as evidenced by their respective absorbance spectra (Figure S6 in the Supporting Information), but is unlikely to be the only one. There are several other possible considerations. The small metallic Pd_4S regions may have a raised Fermi level[38] which would favor electron transfer to water. Additionally, there is less Pd_4S surface exposed to solution near the CdS-Pd_4S interface for the large Pd_4S regions than with small tips. This may increase electron/hole recombination at the CdS-Pd_4S interface over electron transfer to water.

We reported the synthesis of two types of new hybrid nanoparticles containing the semiconductor CdS and the palladium compounds PdO and Pd_4S. CdS-Pd_4S was formed through a high-temperature reduction and simultaneous cation-exchange mechanism. The CdS-PdO hybrids were prepared through aqueous phase hydrolysis and condensation of a palladium precursor and subsequent heterogeneous nucleation of PdO onto the nanorods. These new hybrids undergo photoinduced charge separation, as evidenced by the photoreduction of water. Both show potential as functional hybrid nanoparticles for which increased chemical stability over palladium(0) is required.

Received: October 12, 2010
Published online: December 23, 2010

Keywords: nanoparticles · palladium · photochemistry · semiconductors · water splitting

[1] R. Costi, A. E. Saunders, U. Banin, *Angew. Chem.* **2010**, *122*, 4996–5016; *Angew. Chem. Int. Ed.* **2010**, *49*, 4878–4897.
[2] J. Maynadié, A. Salant, A. Falqui, M. Respaud, E. Shaviv, U. Banin, K. Soulantica, B. Chaudret, *Angew. Chem.* **2009**, *121*, 1846–1849; *Angew. Chem. Int. Ed.* **2009**, *48*, 1814–1817.
[3] L. Amirav, A. P. Alivisatos, *J. Phys. Chem. Lett.* **2010**, *1*, 1051–1054.
[4] J. S. Choi, Y. W. Jun, S. I. Yeon, H. C. Kim, J. S. Shin, J. Cheon, *J. Am. Chem. Soc.* **2006**, *128*, 15982–15983.
[5] M. T. Sheldon, P. E. Trudeau, T. Mokari, L. W. Wang, A. P. Alivisatos, *Nano Lett.* **2009**, *9*, 3676–3682.
[6] J. Zhang, X. H. Liu, X. Z. Guo, S. H. Wu, S. R. Wang, *Chem. Eur. J.* **2010**, *16*, 8108–8116.
[7] S. L. He, H. W. Zhang, S. Delikanli, Y. L. Qin, M. T. Swihart, H. Zeng, *J. Phys. Chem. C* **2009**, *113*, 87–90.
[8] W. L. Shi, H. Zeng, Y. Sahoo, T. Y. Ohulchanskyy, Y. Ding, Z. L. Wang, M. Swihart, P. N. Prasad, *Nano Lett.* **2006**, *6*, 875–881.
[9] G. Menagen, J. E. Macdonald, Y. Shemesh, I. Popov, U. Banin, *J. Am. Chem. Soc.* **2009**, *131*, 17406–17411.
[10] a) T. Mokari, C. G. Sztrum, A. Salant, E. Rabani, U. Banin, *Nat. Mater.* **2005**, *4*, 855–863; b) A. Figuerola, M. van Huis, M. Zanella, A. Genovese, S. Marras, A. Falqui, H. W. Zandbergen, R. Cingolani, L. Manna, *Nano Lett.* **2010**, *10*, 3028–3036.

[11] G. Dukovic, M. G. Merkle, J. H. Nelson, S. M. Hughes, A. P. Alivisatos, *Adv. Mater.* **2008**, *20*, 4306 – 4311.
[12] E. Elmalem, A. E. Saunders, R. Costi, A. Salant, U. Banin, *Adv. Mater.* **2008**, *20*, 4312 – 4317.
[13] M. Berr, A. Vaneski, A. S. Susha, J. Rodríguez-Fernández, M. Döblinger, F. Jäckel, A. L. Rogach, J. Feldmann, *Appl. Phys. Lett.* **2010**, *97*, 093108.
[14] S. E. Habas, P. D. Yang, T. Mokari, *J. Am. Chem. Soc.* **2008**, *130*, 3294 – 3295.
[15] T. Mokari, E. Rothenberg, I. Popov, R. Costi, U. Banin, *Science* **2004**, *304*, 1787 – 1790.
[16] G. Menagen, D. Mocatta, A. Salant, I. Popov, D. Dorfs, U. Banin, *Chem. Mater.* **2008**, *20*, 6900 – 6902.
[17] a) A. Figuerola, I. R. Franchini, A. Fiore, R. Mastria, A. Falqui, G. Bertoni, S. Bals, G. Van Tendeloo, S. Kudera, R. Cingolani, L. Manna, *Adv. Mater.* **2009**, *21*, 550 – 554; b) A. Salant, E. Amitay-Sadovsky, U. Banin, *J. Am. Chem. Soc.* **2006**, *128*, 10006 – 10007.
[18] R. Costi, A. E. Saunders, E. Elmalem, A. Salant, U. Banin, *Nano Lett.* **2008**, *8*, 637 – 641.
[19] N. Z. Bao, L. M. Shen, T. Takata, K. Domen, *Chem. Mater.* **2008**, *20*, 110 – 117.
[20] Y. Ozawa, Y. Tochihara, M. Nagai, S. Omi, *Chem. Eng. Sci.* **2003**, *58*, 671 – 677.
[21] L. M. T. Simplício, S. T. Brandão, E. A. Sales, L. Lietti, F. Bozon-Verduraz, *Appl. Catal. B* **2006**, *63*, 9 – 14.
[22] T. L. Stuchinskaya, I. V. Kozhevnikov, *Catal. Commun.* **2003**, *4*, 417 – 422.
[23] a) Y. H. Ma, I. P. Mardilovich, E. E. Engwall, *Adv. Membrane Technol.* **2003**, *984*, 346 – 360; b) B. D. Morreale, B. H. Howard, O. Iyoha, R. M. Enick, C. Ling, D. S. Sholl, *Ind. Eng. Chem. Res.* **2007**, *46*, 6313 – 6319; c) M. V. Mundschau, X. Xie, C. R. Evenson, A. F. Sammells, *Catal. Today* **2006**, *118*, 12 – 23.
[24] B. Radha, G. U. Kulkarni, *Adv. Funct. Mater.* **2010**, *20*, 879 – 884.
[25] J. J. Bladon, A. Lamola, F. W. Lytle, W. Sonnenberg, J. N. Robinson, G. Philipose, *J. Electrochem. Soc.* **1996**, *143*, 1206 – 1213.
[26] a) W. W. Yu, X. G. Peng, *Angew. Chem.* **2002**, *114*, 2474 – 2477; *Angew. Chem. Int. Ed.* **2002**, *41*, 2368 – 2371; b) L. Carbone, et al., *Nano Lett.* **2007**, *7*, 2942 – 2950.
[27] E. H. Voogt, A. J. M. Mens, O. L. J. Gijzeman, J. W. Geus, *Surf. Sci.* **1996**, *350*, 21 – 31.
[28] Y. S. Bi, G. X. Lu, *Appl. Catal. B* **2003**, *41*, 279 – 286.
[29] K. M. Wang, T. Huang, H. F. Liu, Y. X. Zhao, H. M. Liu, C. T. Sun, *Colloids Surf. A* **2008**, *325*, 21 – 25.
[30] M. M. Hyland, G. M. Bancroft, *Geochim. Cosmochim. Acta* **1990**, *54*, 117 – 130.
[31] J. B. Miller, D. R. Alfonso, B. H. Howard, C. P. O'Brien, B. D. Morreale, *J. Phys. Chem. C* **2009**, *113*, 18800 – 18806.
[32] B. Sadtler, D. O. Demchenko, H. Zheng, S. M. Hughes, M. G. Merkle, U. Dahmen, L. W. Wang, A. P. Alivisatos, *J. Am. Chem. Soc.* **2009**, *131*, 5285 – 5293.
[33] J. M. Luther, H. M. Zheng, B. Sadtler, A. P. Alivisatos, *J. Am. Chem. Soc.* **2009**, *131*, 16851 – 16857.
[34] A. Zubkov, T. Fujino, N. Sato, K. Yamada, *J. Chem. Thermodyn.* **1998**, *30*, 571 – 581.
[35] a) P. D. Burton, D. Lavenson, M. Johnson, D. Gorm, A. M. Karim, T. Conant, A. K. Datye, B. A. Hernandez-Sanchez, T. J. Boyle, *Top. Catal.* **2008**, *49*, 227 – 232; b) S. G. Kwon, T. Hyeon, *Acc. Chem. Res.* **2008**, *41*, 1696 – 1709.
[36] C. R. Bullen, P. Mulvaney, *Nano Lett.* **2004**, *4*, 2303 – 2307.
[37] M. Valden, X. Lai, D. W. Goodman, *Science* **1998**, *281*, 1647 – 1650.
[38] W. P. Zhou, A. Lewera, R. Larsen, R. I. Masel, P. S. Bagus, A. Wieckowski, *J. Phys. Chem. B* **2006**, *110*, 13393 – 13398.

